Finite element and design code assessment of reinforced concrete haunched beams

Mehmet Eren Gulsan[*1], Hasan M. Albegmprli[2a] and Abdulkadir Cevik[1b]

[1]*Civil Engineering Department, Gaziantep University, University Avenue-Central Campus, Gaziantep, Turkey*
[2]*Department of Building & Construction Engineering, Northern Technical University, Engineering Technical College of Mosul, Iraq*

Abstract. This pioneer study focuses on finite element modeling and numerical modeling of three types of Reinforced Concrete Haunched Beams (RCHBs). Firstly, twenty RCHBs, consisting of three types, and four prismatic beams which had been tested experimentally were modeled via a nonlinear finite element method (NFEM) based software named as, ATENA. The modeling results were compared with experimental results including load capacity, deflection, crack pattern and mode of failure. The comparison showed a good agreement between the results and thus the model used can be effectively used for further studies of RCHB with high accuracy. Afterwards, new mechanism modes and design code equations were proposed to improve the shear design equation of ACI-318 and to predict the critical effective depth. These equations are the first comprehensive formulas in the literature involving all types of RCHBs. The statistical analysis showed the superiority of the proposed equation to their predecessors where the correlation coefficient, R^2 was found to be 0.89 for the proposed equation. Moreover, the new equation was validated using parametric and reliability analyses. The parametric analysis of both experimental and predicted results shows that the inclination angle and the compressive strength were the most influential parameters on the shear strength. The reliability analysis indicates that the accuracy of the new formulation is significantly higher as compared to available design equations and its reliability index is within acceptable limits.

Keywords: haunched beam; reinforced concrete; finite element; shear capacity; design code

1. Introduction

The nonlinear finite element analysis is one of the most efficient approaches as a potential numerical method to predict and understand the mechanical behavior of the reinforced concrete members as well as the failure type, crack propagation and stress distribution which are difficult to measure in the experiment. There are some experimental studies related with RCHBs carried out several researchers (Zanuy *et al.* 2015, Hans *et al.* 2013, Tena-Colunga *et al.* 2017a, b, Albegmprli 2017, Tena-Colunga *et al.* 2008). However, studies about the numerical and finite element modeling of RCHBs are very limited. A study provided by Albegmprli *et al.* (2015) discussed the stochastic finite element based reliability analysis of RCHBs. The authors proved that the RCHBs have higher sensitivity and probability of failure than the RC prismatic beams. Yuksel and Yarar (2015) investigated the prediction of load and moment capacity of symmetric parabolic haunched beams due to temperature changes by artificial neural network and adaptive neuro fuzzy inference systems.

Finite element modeling of reinforced concrete

haunched beams designed to fail in shear was investigated by Godinez-Dominguez *et al.* (2015). Design of reinforced concrete haunched beams with respect to American Concrete Institute (ACI) code was assessed by Rombach *et al.* (2011).

This study investigates the finite element and numerical modeling of the simply supported RCHBs. Finite element models were prepared by taking RCHBs that had been tested by Albegmprli (2017) into consideration. Special nonlinear finite element based software named as, ATENA 2D was used to simulate the behavior of the tested RCHBs. The aims of the study are to investigate the effectiveness of the finite element model used for RCHB and to produce new mechanical models and design formula to predict the shear strength of RCHBs with higher accuracy.

The experimental work carried out by Albegmprli (2017) includes twenty-four beams consisting of four prismatic and twenty haunched beams. These beams are classified into three groups depending on the inclination type. Eighteen beams were without stirrups and so collapsed in shear, while other beams were reinforced by shear stirrups and failed in flexure. All of the beams are simply supported have; total length 1700 mm and span 1500 mm, shear span ratio (a/d>2.5) and width 150 mm. However, the values of the inclination angles were 0°, 4.96^o, 9.86^o and 14.62^o. Properties of the materials and geometries of each beam are stated in Table 1.

This paper is composed of three parts. The first part indicates the nonlinear finite element modeling of the experimentally tested RCHBs. Load capacity, load-

---

*Corresponding author, Assistant Professor
  E-mail: gulsan@gantep.edu.tr
[a]Lecturer
  E-mail: albegmprli@ntu.ed.iq
[b]Professor
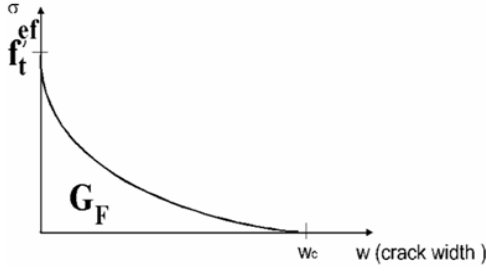 E-mail: akcevik@gantep.edu.tr

Fig. 1 Exponential tension softening

Fig. 2 Concrete compression model

deflection curve, and crack propagation results of finite element analysis are compared with the corresponding experimental results to discuss the effectiveness of the model. In the second part, a new comprehensive design formula is proposed to predict the shear capacity of all types of RCHBs with higher accuracy. In the last part, generalization capability of the proposed formula is investigated by parametric studies and reliability analysis.

2. Theoretical concepts of finite element modeling

2.1 Models of materials

In this study, ATENA 2D software was used to model and simulate the behavior of RCHBs. The plain concrete is modeled using SBETA material model which is available in the software (Cervenka *et al.* 2016). The model includes the non-linear behavior of the concrete in compression. Fracture of concrete in tension is based on the nonlinear fracture mechanics and takes reduction of compressive strength after cracking, biaxial strength failure criterion, tension stiffening and reduction of the shear stiffness after cracking into consideration.

The behavior of concrete in tension and compression is defined by equivalent uniaxial law proposed by Chen and Saleeb (2013). According to the law, the strain, ε_{eq}, is produced by the uniaxial stress σ_{ci} (tensile or compressive) with modulus of elasticity E_{ci}, which is associated with direction i. The relation between the equivalent strain and stress is expressed in Eq. (1). The complete equivalent stress-strain relationship for the concrete was proposed by Chen and Saleeb (2013). The behavior of concrete in tension is divided into two intervals, before and after cracking. The concrete without cracks is assumed to behave as behave linear elastic material and the model is expressed according to the second part of Eq. (1). In this equation, $f_t^{'ef}$ represents the effective tensile strength of the concrete that is obtained from biaxial failure criterion.

$$\varepsilon_{eq} = \frac{\sigma_{si}}{E_c}; \ \sigma_c = E_c \varepsilon^{eq}, 0 \le \sigma_c \le f_t^{'ef} \tag{1}$$

Since, the mechanical behavior changes after cracking, the crack opening in tension is modeled by a fictitious crack model based on a crack-opening law and fracture energy. The model derived by Hordijk (1991) was used to model the concrete after cracking. The model is expressed in Eq.
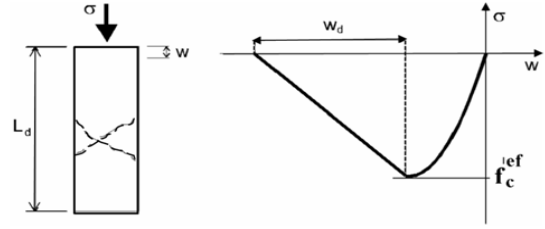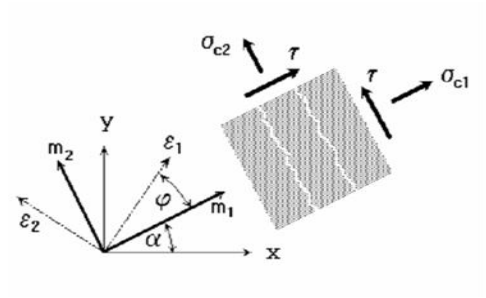

Fig. 3 Fixed crack model

(2). In this equation, w and w_c represents the crack width and crack width after release of all stress, respectively. This formula gives reasonable and better results for the prediction of the crack propagation in concrete (Fig. 1).

$$\frac{\sigma}{f_t^{'ef}} = \left\{ 1 + (c_1 \frac{w}{w_c})^3 \right\} \exp\left(-c_2 \frac{w}{w_c} \right) - \frac{w}{w_c}(1 + c_1^3)$$

$$\exp(-c_2); w_c = 5.14 \frac{G_f}{f_t^{'ef}}; c_1 = 3; c_2 = 6.93 \tag{2}$$

CEB-FIP Model Code 90 is used for modeling the concrete in descending part of the compressive stress- strain relationship, as shown in Fig. 2. The recommended formula in the current model is expressed in Eq. (3). In the equation, x is normalized strain; k is shape parameter and generally can be taken as 1 or higher. The model is appropriate for normal as well as high strength concrete.

$$\sigma_c^{ef} = f_c^{'ef} \frac{kx - x^2}{1 + (k-2)x}, x = \frac{\varepsilon}{\varepsilon_c}, k = \frac{E_o}{E_c} \tag{3}$$

Furthermore, the crack propagation is determined according to the rule that the principle axis is assumed to be fixed in the principle direction at moment of crack initiation, which is the condition of fixed crack model and shown in Fig. 3. The shear strength of the concrete is considered according to the smeared crack model. The shear modulus reduces as normal strain to the crack grows. The shear stiffness reduction due to the crack opening is shown in Fig. 4. The smeared crack approach for modeling of the cracks is adopted in the model SBETA.

The stress-strain relation of the one-dimensional reinforcement is modeled using bilinear law, in other words, elastic-perfectly plastic behavior. The above described stress-strain laws can be used for the discrete as well as the smeared reinforcement.
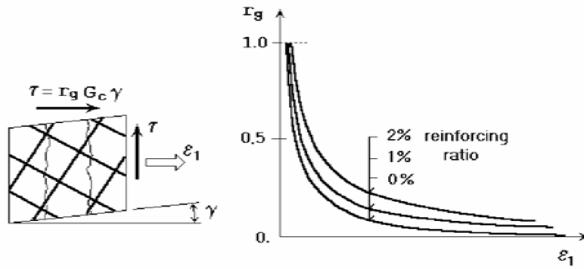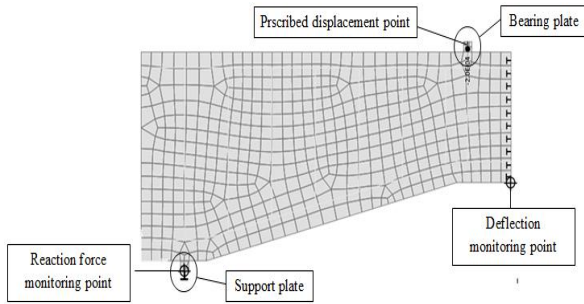
Fig. 4 Shear retention factor

Fig. 6 Load-deflection graph of A1-0 beam

Fig. 5 Finite element modeling in ATENA

Fig. 7 Load-deflection graph of B3-1 beam

3. FE Modeling of beams

All of the experimentally tested beams are symmetric. Therefore, only half of beams were modeled to reduce the total number of the elements for time and memory space saving. Furthermore, the element size was unified along the beam. The support and load bearing plate were modeled by isotropic steel plates which account for steel roller in the experiment. The constraint boundary conditions are necessary to provide the stability and equilibrium in the model. Therefore, the displacement of the symmetry line was prevented to move horizontally and the supporting plate was prevented to move vertically as shown in Fig. 5. The material properties and the geometries of each beam were taken the same as in the experiments for the modeling process.

The assigned loading criteria were very similar to the experimental loading procedure in which prescribed displacement increments are applied in the position of the loading point. The prescribed displacement increment was 0.2 mm at each step. The results of analyses were recorded at specified monitoring points which correspond to the place of measurements in the laboratory experiments. As solution procedure, the analyses were carried out according to Newton-Raphson method.

Fig. 8 Load-deflection graph of C1-0 beam
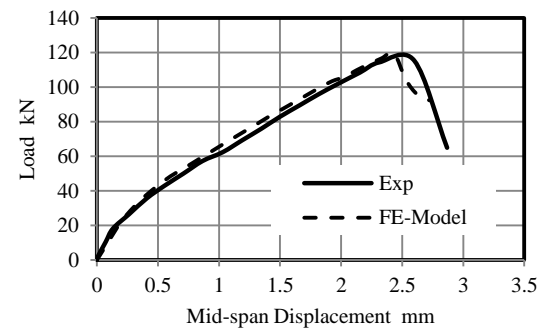
Fig. 9 Load-deflection graph of A2-1 beam

4. Finite element analysis results

The nonlinear finite element analysis results include; failure load, displacement at failure load, load-deflection curve, and crack patterns. The results for monitoring points were recorded and displayed after each step of analysis by the post-processor of the software. This part presents the comparison between the analyses and the experimental results.

4.1 Load capacity and displacement

The results of finite element analyses and the experimental study are presented in Table 1. The comparison includes the load capacity and the displacement. The displacement was compared according to formation of first diagonal shear crack for specimens

Fig. 10 Load-deflection graph of C2-1 beam

Fig. 11 Load-deflection graph of B2-0 beam

Fig. 12 Load-deflection graph of C2-2 beam

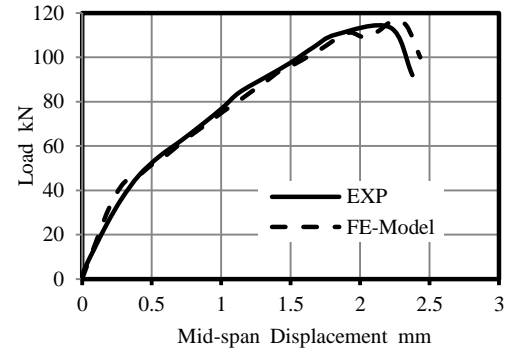Fig. 13 Load-deflection graph of B1-0 beam

Fig. 14 Load-deflection graph of A0-0 beam

Fig. 15 Load-deflection graph of B2-1 beam

Fig. 16 Load-deflection graph of C3-0 beam

Fig. 17 Load-deflection graph of C2-0 beam

without stirrups and it was compared according to yielding point on load-deflection curves for specimens with stirrups. The calculated values by the NFEA exhibit a good agreement with the experimental results. The ratio of the

experimental load capacity to the capacity resulted from the analysis varies between 0.97-1.06, with average 1.01, and

Table 1 Finite element modeling results of experimentally tested beams

Code	α^o	$h_s{}^a$ mm	$h_m{}^b$ mm	A_s mm²	$A_s{}_{,,}$ mm²	$\rho_v{}^c$ 10^{-3}	f_c MPa	F_{exp} kN	F_{pred} kN	$\dfrac{F_{exp}}{F_{pred}}$	W_{exp} mm	W_{pred} mm	$\dfrac{W_{exp}}{W_{pred}}$
A0-0	0	300	300	603	100	-	44.5	53.5	55.3	0.97	1.8	1.9	0.95
A0-2	0	300	300	603	100	6.7	58	107.5	105.5	1.02	4.3	4.7	0.92
A1-0	4.97	300	250	603	100	-	60	56.75	58.15	0.98	2.22	2.23	0.99
A2-0	9.87	300	200	603	100	-	49	56.6	57.95	0.98	2.5	2.18	1.14
A2-1	9.87	300	200	603	308	-	51.5	57.65	59.7	0.97	2.433	2.6	0.94
A2-2	9.87	300	200	603	100	6.7	59	107.5	105.9	1.02	4.53	4.39	1.03
A3-0	14.62	300	150	603	100	-	42.5	60.5	59.05	1.02	2.54	2.52	1.01
A3-1	14.62	300	150	603	308	-	60	56.5	59.5	0.95	3.22	3.6	0.89
A3-2	14.62	300	150	603	100	6.7	59.9	112.5	108	1.04	4.82	4.72	1.02
B0-0	0	300	300	603	100	-	55	55.15	54.7	1.01	1.96	1.84	1.07
B1-0	4.97	300	250	603	100	-	53.5	54.1	54.9	0.99	1.9	1.39	1.37
B2-0	9.87	300	200	603	100	-	55.1	58.5	55.3	1.06	2.24	2.16	1.04
B2-1	9.87	300	200	402	100	-	53.9	45.5	46	0.99	2.57	2.733	0.94
B3-0	14.62	300	150	603	100	-	59.5	66	61.75	1.07	4.64	3.43	1.35
B3-1	14.62	300	150	402	100	-	51.5	61.5	59	1.04	4.57	4.23	1.08
B3-2	14.62	300	150	603	100	6.7	59	104	105	0.99	5.97	5.08	1.17
C0-0	0	250	250	603	100	-	60.7	47.2	46.8	1.01	2.62	2.54	1.03
C1-0	-4.97	300	250	603	100	-	58.5	54	51	1.06	5.55	5.56	0.99
C2-0	-9.87	350	250	603	100	-	44	50.5	52	0.97	5.74	6.06	0.95
C2-1	-9.87	350	250	402	100	-	61	45.9	45.7	1.00	6.53	6.66	0.98
C2-2	-9.87	350	250	603	100	6.7	65	87.5	82.5	1.06	5.4	5.4	1
C3-0	-14.62	400	250	603	100	-	62	52	53.5	0.97	5.33	6.3	0.85
C3-1	-14.62	400	250	402	100	-	50.1	47.75	47.05	1.01	5	4.66	1.07
C3-2	-14.62	400	250	603	100	6.7	59	82.5	78.5	1.05	5.5	6.5	0.85
Average										1.01			1.026
COV										0.03			0.12

$^a h_s$ is the depth of the support; $^b h_m$ is the depth of the mid-span; ^{c} Stirrups by 8 mm diameter at each 100 mm

the same ratio for the deflection at mid-span is found to be between 0.85-1.17, with average 1.026.

4.2 Load-deflection curves

Load-deflection curves of some of the beams resulted from the numerical results versus ones of the experimental study are shown in Figs. 6-22. In general, a noticeable good fit is observed between the curves of experimental and numerical studies. Moreover, better fit is observed between experimental and numerical load-deflection curves of the beams without stirrups till the first diagonal shear crack appears. According to the corresponding figures, the beams of mode A and B fail suddenly due to the diagonal shear crack, the beams C1-0, C2-0, C2-1 & C3-1 have an early diagonal shear crack and continue to carry higher loads as observed from the experimental results. The numerical curve after the first diagonal shear crack could not achieve compatibility with the experimental curve in some specimens, since results were extracted from only half of the beams in the numerical analysis. However, the failure of experimentally tested beams was unsymmetrical in both halves of the beams. All of the beams which were reinforced by stirrups failed in flexure. Almost exact match is observed between the numerical and experimental curves. A reasonable good correlation also exists between numerical and experimental curves for the post-peak region.

4.3 Crack patterns

The crack pattern reflects the mechanical behavior and failure type of concrete members, especially the cracks which cause the failure are significant to research. In this study, the formation, propagation and orientation of the cracks were determined according to the stress and strain values in the integration points of the elements after each step of the analysis. The numerically predicted diagonal shear cracks versus the experimentally observed ones for the RCHBs without shear reinforcement are illustrated in Fig. 22. In the figure, major crack patterns after failure are compared.

The diagonal shear cracks formed suddenly without any indication before the failure in the experimental test and these cracks were usually to be extensive. As a result of the numerical analysis, the shear cracks occurred at the
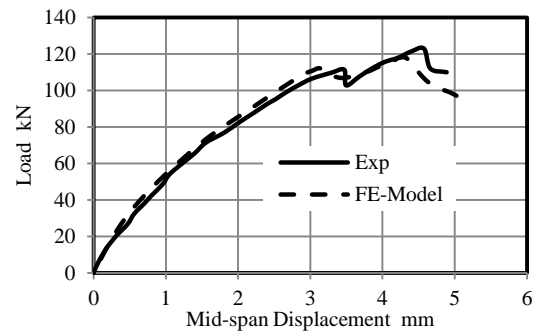
Fig. 18 Load-deflection graph of C3-1 beam

Fig. 19 Load-deflection graph of B3-2 beam
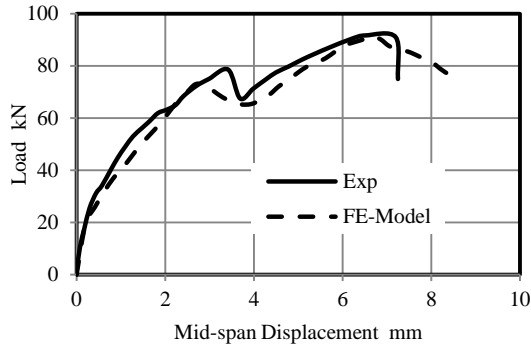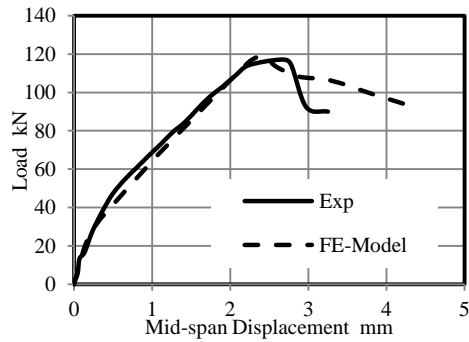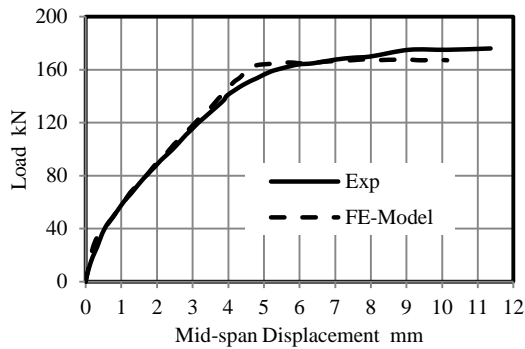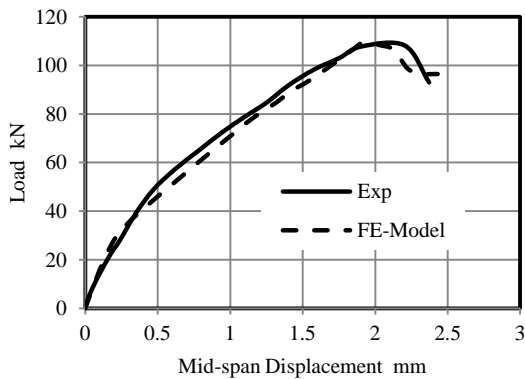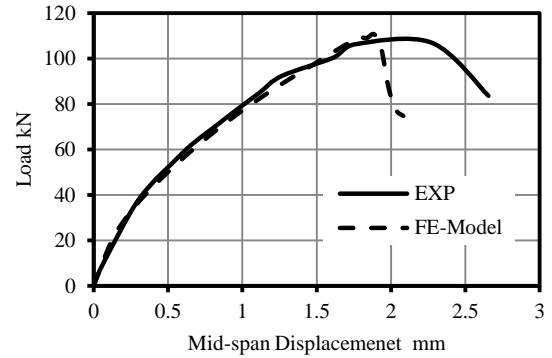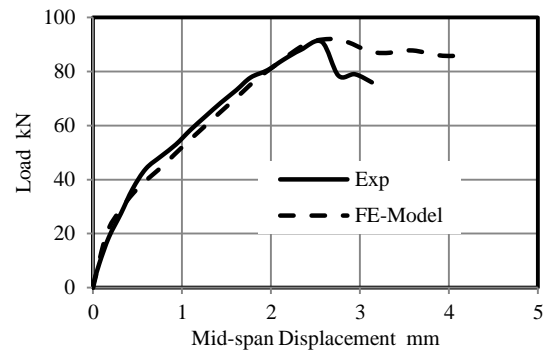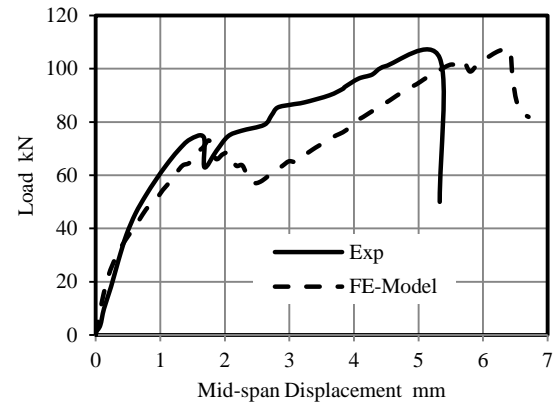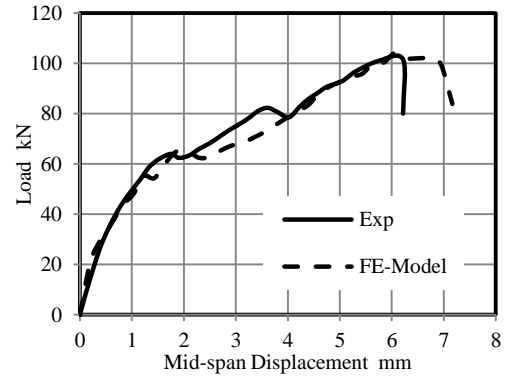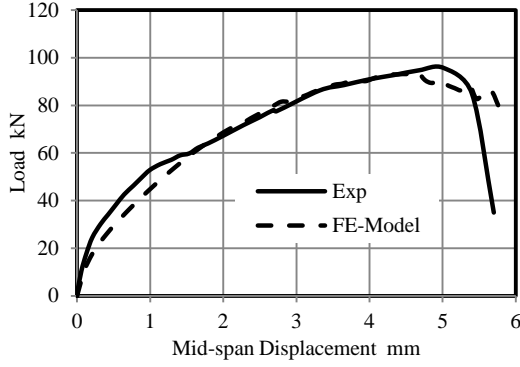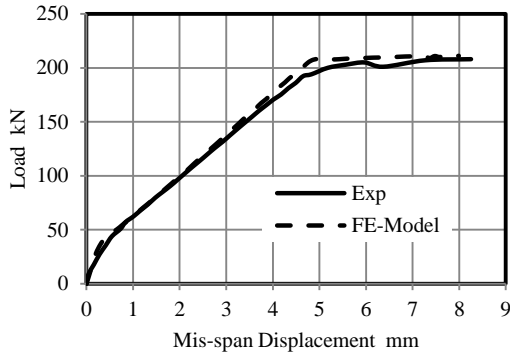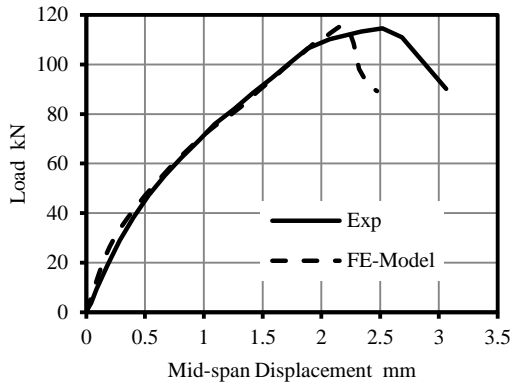

Fig. 20 Load-deflection graph of A2-0 beam
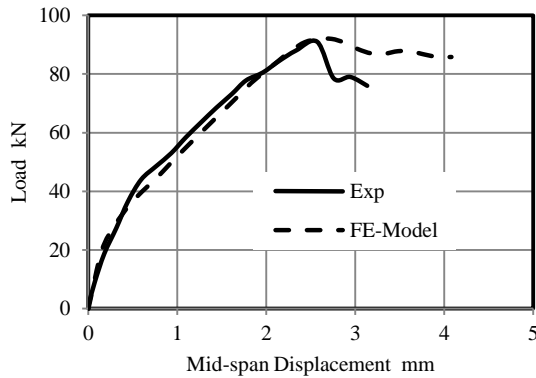
Fig. 21 Load-deflection graph of A3-0 beam

integration points of each adjacent element formed a bundle of cracks along the failure path. The resulted crack patterns

show a reasonable agreement between the numerical and the experimental studies about the orientation and the position of the shear cracks as shown in Fig. 22.

5. Shear capacity models for RCHBs

5.1 Existing formulations

Although RCHBs are widely used in reinforced concrete structures, most design codes do not offer any instructions for design of the beams except the ACI code and the German DIN code. The sections 22.5.1.9 and R22.5.1.9 of ACI 318-14 (2014) point out the variable depth members. These sections confirm to consider the effect of inclined flexural compression in calculating the shear strength of concrete where the internal shear at any section is increased or decreased by the vertical component of inclined flexural stresses. The section 27.4.5.3 of ACI 318-14 (2014) discusses the inclined shear crack in the variable depth beams and recommends measuring the depth at the mid-length of the crack. According to the explanations stated above it can be extracted that the code did not provide any formula to calculate the critical depth or to consider the effect of the inclination on the shear strength of variable depth beams.

Debaiky and Elniema (1982) proposed Eq. (4) for the design of RCHBs. The formula is a modification of the ACI-318 code beam equation that is adapted to RCHBs. The modification contributes influence of the depth variation along the beam by the term $1+1.7\tan a$, and influence of the inclined flexural reinforcement.

$$\frac{V}{bd_s} = (0.16\sqrt{f_c} + 17\rho_s \frac{V_u d}{M_u})(1+1.7\tan a)$$
$$+ \rho_v f_y + 0.25\rho_s f_y \sin a \tag{4}$$

The German code DIN 1045-01 (2001) is the only design code that clearly addressed the shear resistance mechanism of RCHBs in detail. On the other hand, the code introduced Eq. (5)-(5b) to design the shear resistance of RCHBs.

$$V_{Ed} = V_{Edo} - V_{ccd} - V_{td} \leq V_{ED}^{\alpha} \tag{5}$$

$$V_{ED}^{a} = 0.1k(100\rho_l f_{ck})^{0.333}bd;$$
$$k = 1 + \sqrt{\frac{200}{d}} \leq 2 \; ; \; \rho_l \leq 0.02 \tag{5a}$$

$$V_{ccd} = \frac{M_{ED}}{0.9d} \cdot \tan\alpha \tag{5b}$$

Where, V_{Ed} is concrete shear resistance, V_{Edo} is shear force, V_{ccd} is shear resistance due to the inclination of the compression chord, V_{td} is shear resistance component of inclined longitudinal tension reinforcements and V_{ED}^{a} is the design value of the shear bearing capacity of haunched beams at design section. Eqs. (4) and (5) are the most
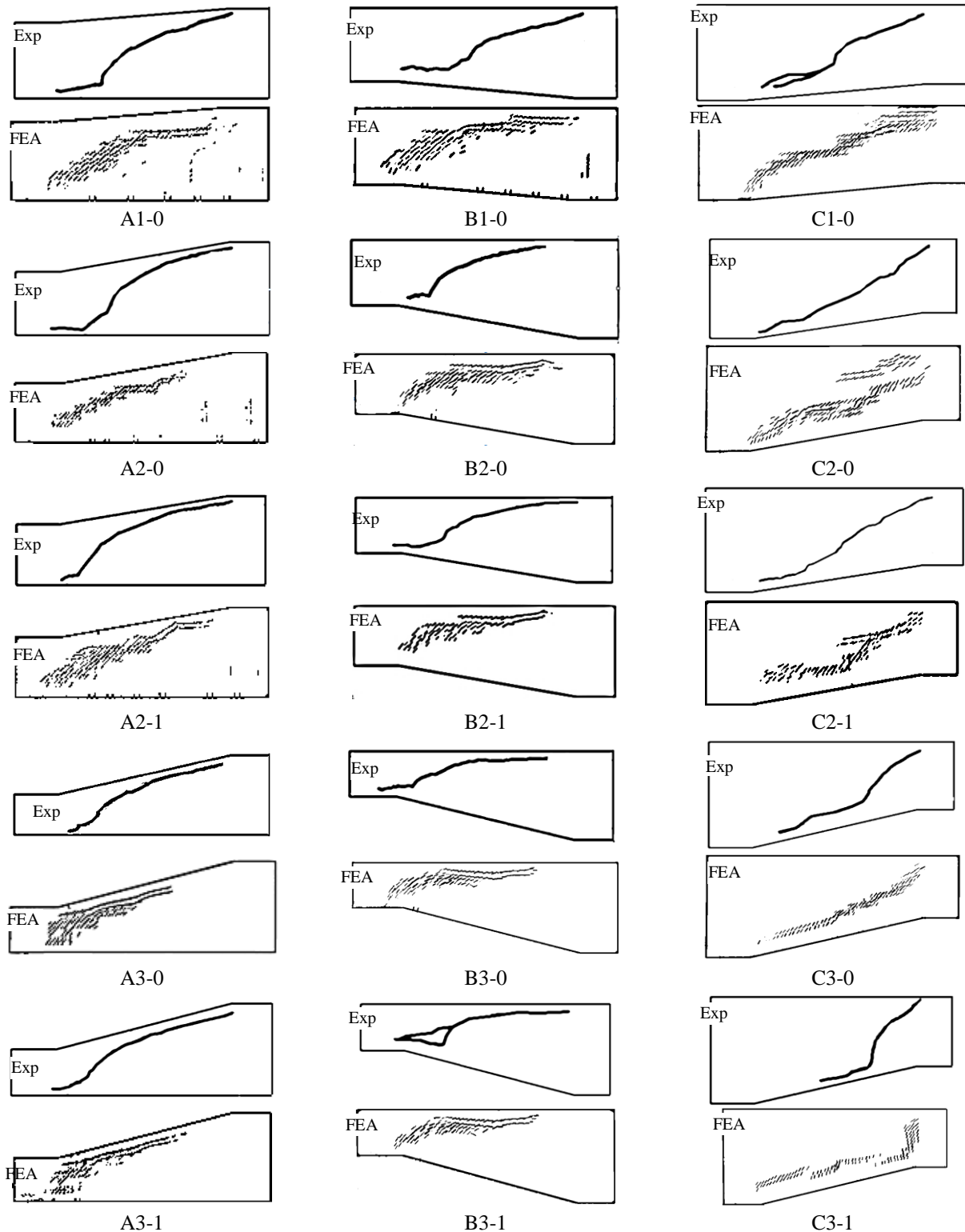
Fig. 22 Comparison of crack patterns between the experimental study and finite element analysis

famous ones in this topic. However, these equations did not consider all cases of RCHBs. Other researchers had their attempts to introduce formulas to predict the shear strength of RCHBs (MacLeod and Houmsi 1994, Tena-Colunga *et al.* 2008). However, these works treated only special cases of the RCHBs and were built on limited data.

5.2 Proposed mechanical models for RCHBs

In this work, three mechanical models (A, B and C) are proposed depending on the inclination type and mechanism of failure as shown in Figs. 23-25. The proposed models differ from each other according to the contribution of the internal stresses; concrete shear resistance (V_C), transverse shear reinforcement (V_v), inclined longitudinal reinforcement (V_F) and compression chord (V_N). The
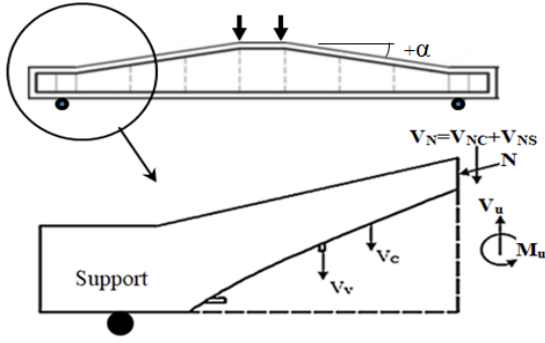
Fig. 23 Mode A
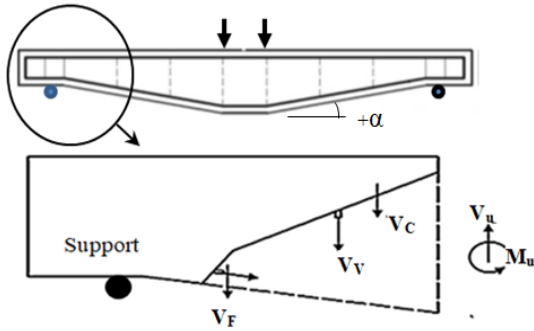
Fig. 24 Mode B
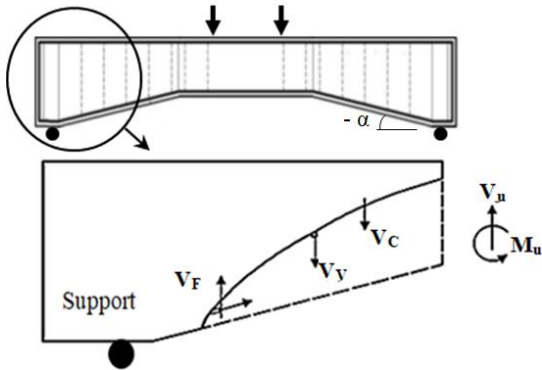
Fig. 25 Mode C

inclination angle is positive in modes A and B and negative in mode C.

5.3 Proposed shear capacity formula for RCHBs

In this study, a new formula was proposed involving all types of RCHBs for the first time in the literature. The new equation consists of four discrete components as stated in Eq. (6). These components represent the contribution of the internal stresses to the proposed mechanical models as are shown Figs. 23-25.

$$V = V_C + V_v + V_N + V_F \qquad (6)$$

Where; V is the ultimate nominal shear strength, V_C is the contribution of the concrete, V_v is the contribution of the shear reinforcement, V_N is the contribution of the compression chord, V_F is the contribution of the inclined flexural reinforcement.

5.3.1 Contribution of the concrete
The contribution of concrete (V_C) in shear is given by the ACI318-14 (2014, Eq. (22.5.5.1a)). This equation predicts the shear strength of the reinforced concrete prismatic beams without shear reinforcement. The equation was modified to Eq. (6a) to involve also RCBHs in which the effective depth was replaced by critical depth (d_c). The parameters ρ, V_u and M_u represent the longitudinal reinforcement ratio, shear force and moment at the critical section, respectively.

$$V_C = (0.16\sqrt{f_c} + 17\rho_c \frac{V_u d_c}{M_u})bd_c \qquad (6a)$$

where, the value of $V_u d_c/M_u$ cannot exceed 1.0.

5.3.2 Contribution of the shear reinforcement
The experimental results did not show a significant effect of shear reinforcement on the capacity of RCHBs. Therefore, the corresponding equation of ACI 318-14 (2014, Eq. (22.5.10.5.3)) was used to calculate the contribution of shear reinforcement to the capacity (V_v), except the effective depth is replaced by the critical effective depth as introduced in Eq. (6b).

$$V_v = \rho_v f_y bd_c \qquad (6b)$$

5.3.3 Contribution of the compression chord
The contribution of the compression chord (V_N) is given in Eq. (6c). This term consists of the vertical components of the normal stress of the concrete and reinforcement bars in the compression chord in the beams of mode A.

$$V_N = \frac{f_c}{20}\left(2bd_c \frac{30}{f_c} + A_{s''}\left(\frac{E_s}{E_c} - 1\right)\right) \cdot \tan\alpha \qquad (6c)$$

The parameters b and d_c are the width and critical depth; respectively, $A_{s''}$ is area of the compression reinforcement, (E_s, E_c) are the modulus of elasticity of concrete and reinforcement; respectively and α is the inclination angle.

5.3.4 Contribution of flexural reinforcement
The contribution of the inclined flexural reinforcement (V_F) is introduced in Eq. (6d). However, the consideration of the inclined flexural reinforcement (A_s) is limited to the modes *B* and *C*. This equation was derived by regression analysis.

$$V_F = 0.2A_s f_y \sin\alpha \qquad (6d)$$

5.3.5 Critical effective depth
The substantial challenge for the design of RCHBs is the determination of the critical effective depth due to variation of depth along the RCHBs. Therefore, a new and practical formulation (Eq. (7)) was proposed to predict the effective depth at critical section by the consideration of the effective depth of the RCHBs on support. The range of the inclination angle lies between -14.62° and +14.62°.
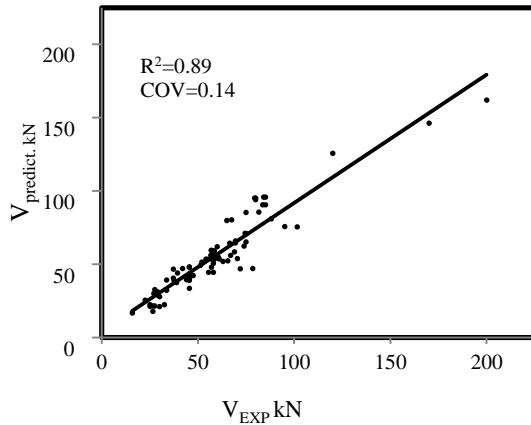
Fig. 26 Correlation of the proposed formula
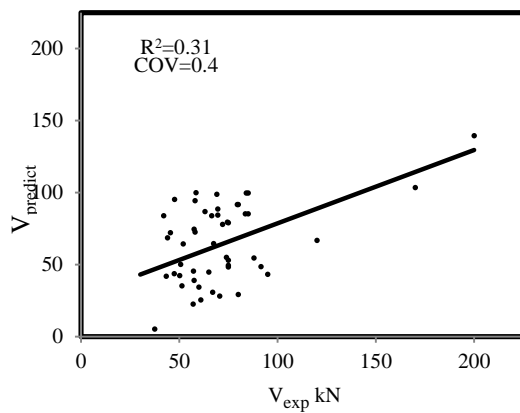
Fig. 27 Correlation of formula proposed by Debaiky and El Neima
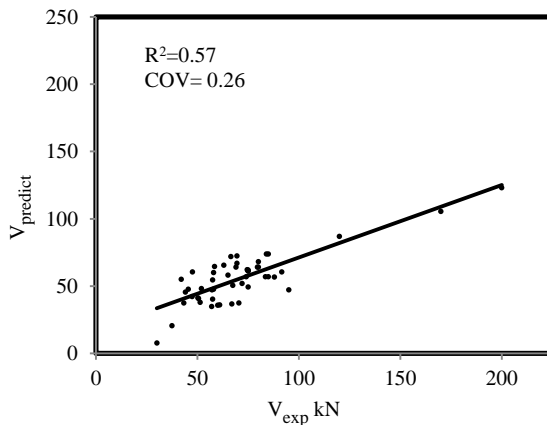
Fig. 28 Correlation of formula proposed by DIN 1045-01

$$F = (1 - 3.04\tan a)^{-0.608} \le 1.55 \qquad (7)$$

Where d_c is the effective depth at the critical section and d_s is the effective depth of the beam on the support.

6. Verification of shear capacity models

6.1 Statistical correlations

The performance of the proposed formula was
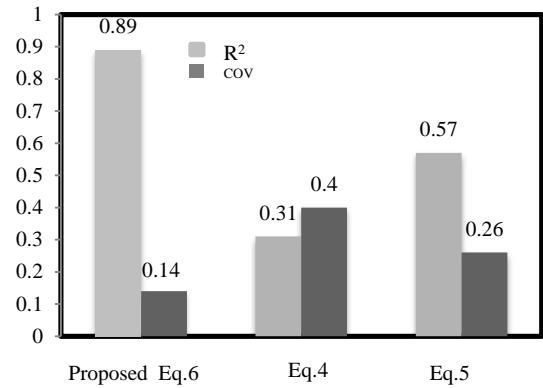
Fig. 29 Comparison of correlation factors between formulas

compared with the other two equations (Eqs. (4) and (5)). The comparisons are shown in Appendix part of the article (Table A.1) and Figs. 26-28. These formulas are the most comprehensive equations for the design of the RCHBs. Table A.1 shows the comparison of the experimental results that obtained from the literature and the predicted nominal shear capacity values of the corresponding beams resulted from the three equations. Furthermore, Figs. 26-28 illustrate the correlation between the experimental results and predicted values. The correlations of the results are represented by the correlation coefficient (R^2) and coefficient of variation (CoV). The correlation factors for the proposed formula, Eq. (6) are $V_{predicted}/V_{test} = 0.96$, CoV=0.14 and $R^2 = 0.89$; for Eq. (4) are $V_{predicted}/V_{test} = 0.81$, CoV=0.4 and $R^2 = 0.31$; and for Eq. (5) are $V_{predicted}/V_{test} = 0.62$, CoV=0.26 and $R^2 = 0.57$. The statistical parameters stated above and comparison of them, as shown in Fig. 29, prove the efficiency and superiority of the proposed design model for all cases of RCHBs.

6.2 Parametric study of the proposed formula

The parametric study was carried out to verify the generalization of the proposed model and to study the influence of each parameter on the predicted value. Parametric study was implemented by the help of Monte Carlo simulation. In addition to values of the parameters of the experimental study, extra database was produced via Monte Carlo simulation according to range and coefficient of variation of each parameter (Table 2). Main effect plots were extracted as a result of the parametric study as shown in Figs. 30-32. The three categories of beams (A, B and C) were examined separately by the parametric analysis. The minimum and maximum values of each parameter were utilized as identified by the experimental database. The considered parameters are; compressive strength (f_c), yield strength of the reinforcement (f_y), longitudinal flexural reinforcement ratio (ρ_s), transverse shear steel ratio (ρ_v) and inclination angle (α).

As a result of the study, it was extracted that the proposed model has high generalization capability for the range of the variables. It can be observed from Figs. 30-32 that all parameters have a significant influence on the shear capacity of the RCHBs. Although the compressive strength
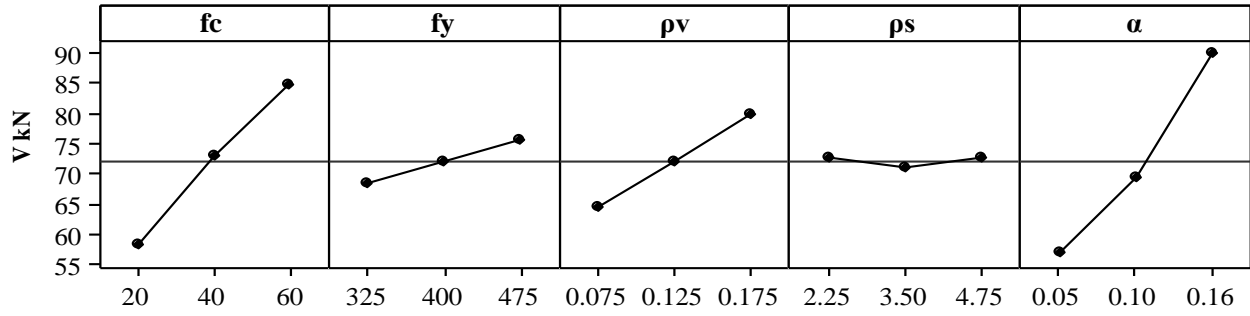
Fig. 30 Parametric study results for Mod A
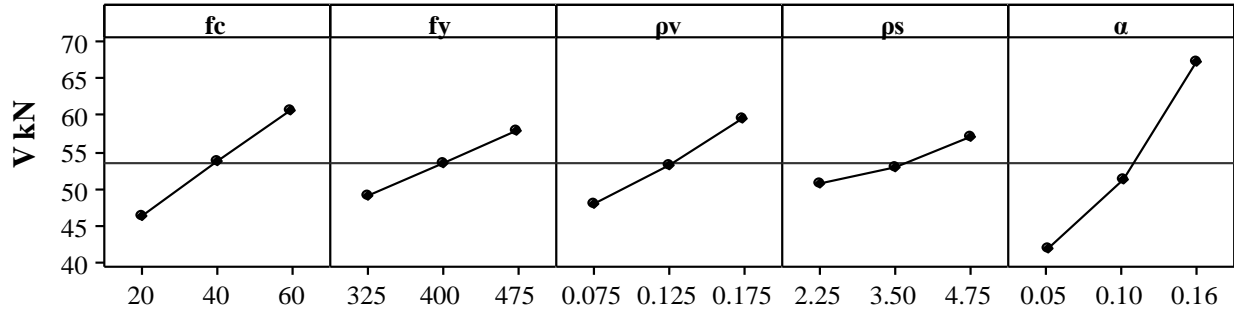
Fig. 31 Parametric study results for Mod B

(f_c) shows a significant influence on the shear capacity, effect of yield strength of steel bars (f_y) is negligibly small for all RCHB types. The shear reinforcement ratio (ρ_v) has also a remarkable effect on the shear strength; especially in Mode C. The flexural reinforcement ratio (ρ_s) has a positivity effect in Modes A&B and negative effect in beams of Mode C as observed in Figs. 30-32. However, influence of the inclination angle (α) is the highest among all considered parameters.

7. Reliability analysis

7.1 Concepts

The material properties and geometric aspects of structural members usually have uncertain values. Therefore, it is difficult to model the real behavior of reinforced concrete members using deterministic analysis. Probabilistic models are required to quantify the uncertainties of the parameters to develop realistic representations of the output and failure state of these systems to obtain a rational and safe design (Vorechovsky 2004). The uncertainty of the parameters is modeled as random variables which described by the probability distribution functions (PDF). Table 2 summarizes the statistical parameters of material properties, member geometries and load factors. The coefficient of variation values of statistical parameters are taken from previous studies (Choi *et al.* 2004, Strauss *et al.* 2006, Szerszen and Novak 2003).

Structural reliability can be defined as the capability of a structure or a structural member to achieve the specified requirements for which it has been designed (EN 1990, 2002). The requirement for a structural element can be

Table 2 Uncertainty factors

Variable	Statistical distribution	Mean	COV
Width, depth and inclination	Normal	Nominal	0.03
Reinforcement effective depth	Normal	Nominal	0.03
Reinforcement area	Normal	Nominal	0.05
Concrete compressive strength	Normal	Nominal	0.1
Concrete modulus of elasticity	Normal	Depends on strength	0.07
Yield strength	Normal	Nominal	0.1
Steel Modulus	Beta	Nominal	0.1
Dead load	Normal	Nominal	0.08
Live load	Normal	Nominal	0.18

achieved when the external applied loads (Q) do not exceed the resistance of the element (R). The corresponding limit state function, g for structural reliability can be expressed in Eq. (8) as follows

$$g = R - Q;$$

$$R = \phi R_n (X_1, X_2, \ldots \ldots, X_n) \& Q = \lambda_D D + \lambda_L L \quad (8)$$

Where X_i represents the random parameters, D is dead load, L is live load, ϕ is reduction factor and λ is bias factor. The reliability of the structure is assessed by the failure probability of limit state function which is given explicitly in Eq. (9).

$$P_f = P(g < 0) \quad (9)$$

7.2 Reliability index

The reliability index is the shortest distance from the
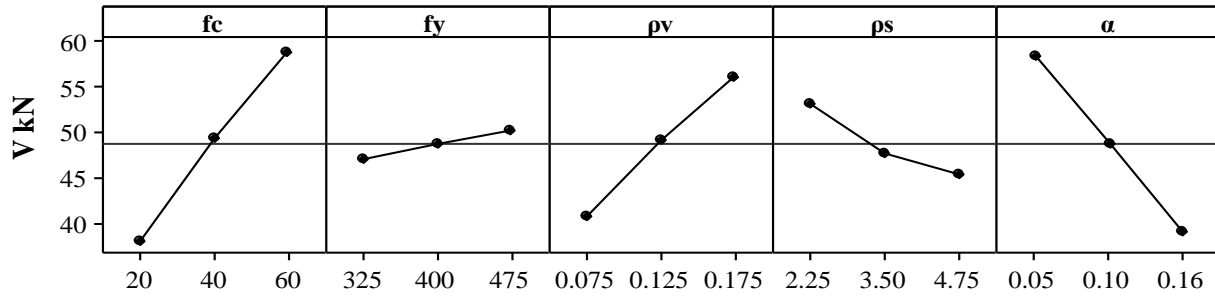
Fig. 32 Parametric study results for Mod C

origin of the reduced variables to the failure surface as introduced by Hasofer and Lind (1974). The reliability index β is strongly related to the probability of failure, Pf, as stated in Eq. (10)

$$\beta = -\phi^{-1}(P_f) \tag{10}$$

Where ϕ^{-1} is the inverse of the probabilistic distribution function, P_f is the failure probability and β is the reliability index. The expression of the reliability index is expressed in Eq. (11)

$$\beta = \frac{\mu_R - \mu_Q}{\sqrt{\sigma_R^2 + \sigma_Q^2}} \tag{11}$$

The reliability analysis was achieved according to the load and resistance factor design (LRFD) approach which is specified by ASCE-7 and ACI 318-14 (Eq. (12)). ϕ represents the strength reduction factor, D and L are dead and live loads, respectively.

$$1.2 \cdot D + 1.6 \cdot L < \phi R$$
$$1.4 \cdot D < \phi R \tag{12}$$

Due to the critical effective depth concept, reinforced concrete haunched beams have more risk as compared to prismatic beams regarding shear forces.

Table 3 shows the reliability indices of the predicted shear strengths from the proposed and existing formulas using the limit state load case in Eq. (12) for three values of strength reduction factors (0.8, 0.75 and 0.7). Calculation procedure of reliability index is same for all considered equations (Eqs. (4), (5) and (6)). The values in Table 3 show reliability indices of each formulation for load ratio (D/D+L) of 0.5. According to the results, reliability indices for the proposed formula are higher than the others. In other words, the proposed formula gives more reliable and safer results for the capacity of RCHBs. Acceptable reliability index values are obtained for the strength reduction value of 0.75. Indeed, this value is also recommended by ACI code for the structural elements which are critical regarding shear. Therefore, the reduction factor of 0.75 is recommended for the application of the proposed formula.

Fig. 33 presents change of the reliability indices of the three formulas according to different load ratios (D/D+L) for strength reduction factor of 0.75.

8. Nominal design capacity

The new formulation is proposed to extend the application
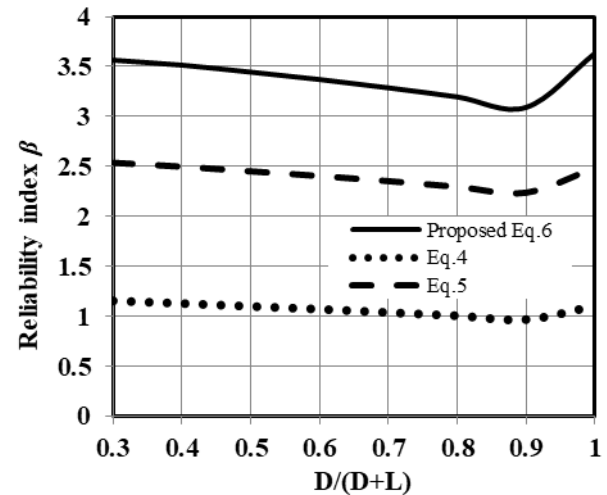
Fig. 33 Reliability index for different ratio of loading (D/D+L)

Table 3 Resulting reliability indices, β

Strength Reduction factor (ϕ)	Eq. (4)	Eq. (5)	Eq. (6) (Proposed Formulation)
0.8	1.04	2.32	3.2
0.75	1.1	2.45	3.45
0.7	1.17	2.59	3.74

of shear design formula which is adopted by ACI318 to involve all types of RCHBs. The proposed formulation adopts the factors based on the Eq. (12) for load combinations and the strength reduction factor, ϕ =0.75. Therefore, nominal design capacities (V_w) are calculated according to Eq. (12). The load ratio of, D/(D+L), 0.5 was considered for the calculation. The nominal design capacities of RCHBs which are resulted from Eqs. (4), (5) and (6) are given in Table A.1. For instance, the nominal design capacity of the beam named as, A1-0 was calculated according to Eq. (6) as follows;

The resulting capacity of the beam resulted from the proposed formulation is 59.62 kN. This value is placed in Eq. (12) (*R*). Since, 0.5 value is considered as D/(D+L) ratio, Nominal design capacity of the beam;

$$\frac{0.75 * 59.62}{(1.2 * 0.5 + 1.6 * 0.5)} = 31.94 kN \tag{13}$$

The safety factor was also determined using the following equation

$$SF = \frac{V_{\exp}}{V_w} \qquad (14)$$

Where, V_{exp} is the experimental shear capacity and V_w is the design capacity. The average values of the safety factor are equal to 2 with COV=0.16 for the proposed formula, 3.35 with COV=1.11 for Eq. (4), and 2.88 with COV=0.68 for Eq. (5). Therefore, it can be concluded that when resulting reliability index, safety factors and COV values are taken into consideration, the proposed formula gives more reliabile and economic results for the design of all types of haunched beams as compared to other formulations.

9. Conclusions

In this study, the experimentally tested RCHBs were modeled by ATENA 2D program to simulate the mechanical behavior of the RCHBs. Also, a new formulation was proposed for the prediction of the shear strength capacity of RCHBs. The noticeable conclusions are summarized as follows:

• The predicted values of the NFEM exhibited a good agreement with the experimental results. The ratio of predicted capacities of RCHB to the corresponding experimental results was found to be in the range of 0.97 – 1.06, with average 1.01. Moreover, the ratio of the predicted result to the experimental result for mid-span deflection at failure load was found to be between 0.85-1.17, with average 1.026.

• A reasonable similarity was observed about the orientation and position of the diagonal shear cracks between the NFEA and the experimental study.

• A comprehensive formulation was proposed for the prediction of failure load and design of all cases of RCHBs and new parameters were taken into account in the equation for the first time in literature.

• The proposed formula exhibited better agreement with the experimental results as compared to the existing design equations for RCHBS.

• The parametric analysis indicated that the proposed model had the capability of determination of the capacity of RCHBs for wide ranges of variables. Moreover, the inclination angle (α) and the compressive strength (f_c) were the most influential parameters on the shear strength of RCHBs.

• As a result of reliability analysis, the safety margin of the proposed model is found to be higher and more reliable as compared to existing design formulas for uncertain material and geometric properties of RCHBs.

• The safety factor of the proposed model for the design of RCHBs is found to be 2.

References

ACI 318 (2014), *Building Code Requirements for Structural Concrete and Commentary*, American Concrete Institute; Farmington Hills, Michigan, U.S.A.

ASCE 7-98 (1998), *Minimum Design Load for Buildings and Other Structures*, Washington, U.S.A.

Albegmprli, H.M., Cevik, A., Gulsan, M.E. and Kurtoglu, A.E. (2015), "Reliability analysis of reinforced concrete haunched beams shear capacity based on stochastic nonlinear FE analysis", *Comput. Concrete*, **15**(2), 259-277.

Albegmprli, H.M. (2017), "Experimental investigation and stochastic FE modeing of reinforced concrete haunched beams", Ph.D. Dissertation, Gaziantep University, Gaziantep, Turkey.

Cervenka, V., Jendele, L. and Cervenka, J. (2016), *ATENA Program Documentation: Theory, Cervenka Consulting*, Prague, Czech Republic.

Cervenka, V. (1985), "Constitutive equations for cracked concrete", *ACI J. Proc.*, **82**(6), 877-882.

Chen, W.F. and Saleeb, A.F. (2013), *Constitutive Equations for Engineering Materials*, Elsevier, Amsterdam, the Netherlands.

Choi, B.S., Scanlon, A. and Johnson, P.A. (2004), "Monte Carlo simulation of immediate and time-dependent deflections of reinforced concrete beams and slabs", *ACI Struct. J.*, **101**(5), 633-641.

Debaiky, S.Y. and El-Niema, E.I. (1982), "Behavior and strength of reinforced concrete haunched beams in shear", *ACI Struct. J.*, **79**(3), 184-194.

DIN 1045-01 (2001), *Tragwerke aus Beton, Stahlbeton und Spannbeton*, Teil 1Bemessungund Konstruktion, Beuth Verlag GmbH, Berlin, Germany.

El-Niema, E.I. (1988), "Investigation of concrete haunched t-beams under shear", *ASCE-J. Struct. Eng.*, **114**(4), 917-930.

EN 1990 (2002), *Basis of Structural Design*, European Committee for Standardization, European Union.

Godinez-Dominguez, E.A., Tena-Colunga, A. and Juarez-Luna, A. (2015), "Nonlinear finite element modeling of reinforced concrete haunched beams desihned to develop a shear failure", *Eng. Struct.*, **105**, 99-122.

Hans, I.A.A., Arturo, T.C. and Alejandro, G.V. (2013), "Behavior of reinforced concrete haunched beams subjected to cyclic shear loading", *Eng. Struct.*, **49**, 27-42.

Hasofer, A.M. and Lind, N.C. (1974), "An exact and invariant second-moment code format", *J. Eng. Mech. Div.*, **100**(1), 111-121.

Hordjik, D.A. (1991), "Local approach to fatigue of concrete", Ph.D. Dissertation, Delft University of Technology, the Netherlands.

MacLeod, I.A. and Houmsi, A. (1994), "Shear strength of haunched beams without shear reinforcement", *ACI Struct. J.,* **91**(1), 79-89.

Nghiep, V.H. (2010), "Shear design of straight and haunched concrete beams without stirrups", Ph.D. Dissertation, Technischen Universitat Hamburg, Hamburg, Germany.

Rombach, G.A., Kohl, M. and Nghiep, V.H. (2011), "Shear design of concrete members without shear reinforcement-a solved problem?", *Proc. Eng.*, **14**, 134-140.

Stefanou, G.D. (1983), "Shear resistance of reinforced concrete beams with non-prismatic section", *Eng. Fract. Mech.*, **18**(4), 643-666.

Strauss, A., Mordini, A. and Bergmeister, K. (2006), "Nonlinear finite element analysis of reinforced concrete corbels at both deterministic and probabilistic levels", *Comput. Concrete*, **3**(2), 123-144.

Szerszen, M.M. and Novak, A.S. (2003), "Calibration of design code of buildings (ACI 318): Part 2-Reliability analysis and resistance factors", *ACI Struct. J.*, **100**(3), 383-391.

Tena-Colunga, A., Urbina-Californias, L.A. and Archundia-Aranda, H.I. (2017a), "Assessment of the shear strength of continous reinforced concrete haunched beams based upon cyclic testing", *J. Build. Eng.*, **11**, 187-204.

Tena-Colunga, A., Urbina-Californias, L.A. and Archundia-Aranda, H.I. (2017b), "Cyclic behavior of continuous reinforced

concrete haunched beams with transverse reinforcement designed to fail in shear", *Constr. Build. Mater.*, **151**, 546-562.

Tena-Colunga, A., Hans, I.A. and Oscar, M.G. (2008), "Behavior of reinforced concrete haunched beam subjected to to static shear loading", *Eng. Struct.*, **30**(2), 478-492.

Vorechovsky, M. (2004), "Stochactic fracture mechanics and size effect", Ph.D. Dissertation, Brno University of Technology, Czech Republic.

Yuksel, S.B. and Yarar, A. (2015), "Neuro-fuzzy and artificial neural networks modeling of uniform temperature effects of symmetric parabolic haunched beams", *Struct. Eng. Mech.*, **56**(5), 787-796.

Zanuy, C., Gallego, J.M. and Albajar, L. (2015), "Fatigue behavior of reinforced concrete haunched beams without stirrups", *ACI Struct. J.*, **112**(3), 371-381.

CC

Abbreviations

a	Shear span
b	Beam width
d_c	Effective depth at the critical section
d_s	The effective depth at the support
D	Dead Load
L	Live Load
E_c	Secant modulus of elasticity
s	Initial elastic modulus
E_s	Elasticity modulus of reinforcement
f_c	Compressive strength of concrete
$f_c^{'ef}$	Concrete effective compressive strength
$f_t^{'ef}$	The effective tensile strength
f_y	Reinforcement yield strength
G^f	The fracture energy
M_u	Moment force at the critical section
V_n	Nominal ultimate shear capacity for considered eqs.
V_u	Shear force at the critical section
V_w	The nominal design capacity for haunched beams
w	The crack opening
w_c	The crack opening at the complete release of stress
α	Inclination angle
ε	Strain
ε_c	Strain at the peak stress
ε^{eq}	The equivalent uniaxial strain
ρ_c	Reinforcement ratio at the critical section
ρ_s	Flexural reinforcement ratio
ρ_v	Shear reinforcement ratio
σ_{ci}	The uniaxial stress
σ^{ef}	The effective tensile stress
σ_c^{ef}	Concrete compressive stress
ϕ	Resistance reduction factor

Appendix

Table A.1 Experimental database of RCHBs and comparison of models

Beam	Mode	a	α	f_c MPa	A_v mm²	A_s mm²	b mm	d_s mm	$A_s^{\cdot\cdot}$ mm	V_{exp} kN	Eq. (6) V_n kN	Bias	V_w kN	Safety factor	Eq. (4) V_n kN	Bias	V_w kN	Safety factor	Eq. (5) V_n kN	Bias	V_w kN	Safety factor
					Albegmprli (2017)																	
A1-0	A	0.65	4.97	60.00	0	603	150	210	100	56.75	59.62	1.05	31.94	1.77	80.11	1.41	42.92	1.32	40.79	0.72	27.19	2.09
A2-0	A	0.65	9.87	49.00	0	603	150	160	100	56.6	55.94	0.99	29.97	1.89	86.10	1.52	46.13	1.23	45.52	0.80	30.35	1.87
A2-1	A	0.65	9.87	51.50	0	603	150	160	308	57.65	57.31	0.99	30.70	1.88	110.97	1.92	59.45	0.97	46.28	0.80	30.85	1.87
A3-0	A	0.65	14.62	52.00	0	603	150	110	100	60.5	55.05	0.91	29.49	2.05	95.98	1.59	51.42	1.18	53.17	0.88	35.45	1.71
A3-1	A	0.65	14.62	46.00	0	603	150	110	308	56.5	53.72	0.95	28.78	1.96	110.85	1.96	59.38	0.95	51.04	0.90	34.03	1.66
					Nghiep (2010)																	
2L1	A	1.5	3.95	49.45	0	942	200	223	0	75	70.80	0.94	37.93	1.98	79.00	1.05	42.32	1.77	62.10	0.83	41.40	1.81
2L2	A	1.5	3.95	49.99	0	942	200	223	0	74.5	71.12	0.95	38.1	1.96	79.40	1.07	42.54	1.75	62.30	0.84	41.53	1.79
3L1	A	1.5	5.91	50.21	0	942	200	178	0	66.5	64.29	0.97	34.44	1.93	93.80	1.26	50.25	1.32	72.10	1.08	48.07	1.38
3L2	A	1.5	5.91	50.98	0	942	200	178	0	69.5	64.66	0.93	34.64	2.01	84.40	1.21	45.21	1.54	72.50	1.04	48.33	1.44
2K1	A	0.85	3.95	54.18	0	942	200	267	0	83.5	90.47	1.08	48.47	1.72	85.30	1.02	45.70	1.83	57.10	0.68	38.07	2.19
2K2	A	0.85	3.95	54.22	0	942	200	267	0	85	90.50	1.06	48.48	1.75	85.30	1.00	45.70	1.86	57.10	0.67	38.07	2.23
3K1	A	0.85	6.71	54.26	0	942	200	238	0	79.5	95.06	1.20	50.93	1.56	91.60	1.15	49.07	1.62	64.20	0.81	42.80	1.86
3K2	A	0.85	6.71	54.31	0	942	200	238	0	80	95.09	1.19	50.94	1.57	91.70	1.15	49.13	1.63	64.20	0.80	42.80	1.87
4K1	A	0.85	10.01	54.78	0	942	200	198	0	85	95.88	1.13	51.36	1.65	99.70	1.17	53.41	1.59	73.80	0.87	49.20	1.73
4K2	A	0.85	10.01	54.78	0	942	200	198	0	84	95.88	1.14	51.36	1.64	99.70	1.19	53.41	1.57	73.80	0.88	49.20	1.71
					MacLeod and Houmsi (1994)																	
B2	A	0.81	4.76	37.90	0	736	150	175	157	45.5	41.22	0.91	22.08	2.06	41.90	0.97	22.45	2.03	37.50	0.87	25.00	1.82
B4	A	0.9	6.36	33.50	0	736	150	175	157	45.5	43.42	0.95	23.26	1.96	50.50	0.99	27.05	1.68	40.90	0.81	27.27	1.67
B5	A	0.81	7.56	35.50	0	736	150	145	157	45.5	39.86	0.88	21.35	2.13	73.70	0.92	39.48	1.15	42.30	0.89	28.20	1.61
B5R	A	0.81	7.56	33.00	0	736	150	145	157	45.5	38.92	0.86	20.85	2.18	42.30	0.84	22.66	2.01	41.30	0.82	27.53	1.65
B6	A	0.81	10.37	33.20	0	736	150	150	157	45.5	48.20	1.06	25.82	1.76	45.40	0.79	24.32	1.87	47.30	0.83	31.53	1.44
					Stefanou (1983)																	
B3- Ia	A	0.6	13.39	15.72	0	226	100	100	100	27.5	21.63	0.79	11.59	2.37	14.77	0.93	7.91	3.48	17.71	0.64	11.81	2.33
B3-Ib	A	0.6	13.39	15.72	0	402	100	100	100	25	22.39	0.90	11.99	2.08	18.45	0.74	9.88	2.53	21.46	0.86	14.31	1.75
B4- Ia	A	0.6	8.13	15.72	0	226	100	150	100	26.5	21.61	0.82	11.58	2.29	16.22	0.61	8.69	3.05	15.47	0.58	10.31	2.57
B4-Ib	A	0.6	8.13	15.72	0	402	100	150	100	32.5	22.47	0.69	12.04	2.7	18.47	0.62	9.89	3.28	18.75	0.58	12.50	2.60
B7- Ias	A	0.6	13.39	15.72	56.55	226	100	100	100	29	30.46	1.05	16.32	1.78	20.59	0.92	11.03	2.63	25.56	0.88	17.04	1.70
B7-Ibs	A	0.6	13.39	15.72	56.55	402	100	100	100	29	31.22	1.08	16.73	1.73	24.27	0.90	13.00	2.23	29.31	1.01	19.54	1.48
B8- Ias	A	0.6	8.13	15.72	56.55	226	100	150	100	27.5	32.76	1.19	17.55	1.57	24.95	0.86	13.37	2.06	26.51	0.96	17.67	1.56
B8-Ibs	A	0.6	8.13	15.72	56.55	402	100	150	100	45.5	33.63	0.74	18.02	2.53	27.19	0.81	14.57	3.12	29.78	0.65	19.85	2.29
					Debaiky and El-Niema (1982)																	
A2	B	0.9	9.46	20.00	47.5	942	120	110	0	58	44.45	0.77	23.81	2.44	72.48	1.25	38.83	1.49	47.73	0.82	31.82	1.82
C2	B	0.9	9.46	28.20	47.5	942	120	110	0	72	46.80	0.65	25.07	2.87	77.85	1.08	41.71	1.73	52.13	0.72	34.75	2.07
D3	B	0.9	9.46	29.60	47.5	942	120	110	0	69	58.40	0.85	31.29	2.21	98.72	1.43	52.89	1.30	64.24	0.93	42.83	1.61
D4	B	0.9	9.46	27.50	100.5	942	120	110	0	58.5	59.15	1.01	31.69	1.85	99.78	1.71	53.45	1.09	64.56	1.10	43.04	1.36
E4	B	0.9	9.46	34.00	56.6	603	120	110	0	42	47.17	1.12	25.27	1.66	83.97	2.00	44.98	0.93	55.25	1.32	36.83	1.14
F3	B	0.9	9.46	21.50	56.55	603	120	110	0	44	39.42	0.90	21.12	2.08	68.46	1.56	36.68	1.20	45.47	1.03	30.31	1.45
F4	B	0.9	9.46	21.00	56.55	763	120	110	0	45.5	42.78	0.94	22.92	1.99	72.15	1.59	38.65	1.18	47.82	1.05	31.88	1.43
A3	B	0.9	4.76	17.80	47.5	942	120	185	0	78.5	47.17	0.60	25.27	3.11	58.38	0.74	31.28	2.51	43.62	0.56	29.08	2.70
E5	B	0.9	4.76	35.50	56.6	603	120	185	0	57.5	59.22	1.03	31.73	1.81	74.50	1.30	39.91	1.44	54.68	0.95	36.45	1.58
C3	B	0.9	4.76	27.80	47.5	942	120	185	0	52	51.55	0.99	27.62	1.88	64.38	1.24	34.49	1.51	48.15	0.93	32.10	1.62

Table A.1 Continued

Debaiky and El-Niema (1982)																						
B3	B	0.7	12.10	18.60	47.5	942	120	110	0	65.5	52.24	0.80	27.99	2.34	40.36	0.62	21.62	3.03	29.07	0.44	19.38	3.38
B4	B	0.5	16.70	21.00	47.5	942	120	110	0	101.5	75.52	0.74	40.46	2.51	49.37	0.49	26.45	3.84	29.79	0.29	19.86	5.11
Stefanou (1983)																						
B1-Ia	B	0.6	13.39	19.99	0	226	100	100	0	15.8	16.68	1.06	8.94	1.77	11.88	0.75	6.36	2.48	9.32	0.59	6.21	2.54
B1-Ib	B	0.6	13.39	19.99	0	402	100	100	0	25	21.22	0.85	11.37	2.2	15.56	0.62	8.34	3.00	11.29	0.45	7.53	3.32
B2- Ia	B	0.6	8.13	19.99	0	226	100	150	0	26.5	17.86	0.67	9.57	2.77	13.61	0.51	7.29	3.63	11.55	0.44	7.70	3.44
B2-Ib	B	0.6	8.13	19.99	0	402	100	150	0	30	21.09	0.70	11.3	2.66	15.86	0.53	8.50	3.53	13.99	0.47	9.33	3.22
B5- Ias	B	0.6	13.39	19.99	56.55	226	100	100	0	22.5	25.51	1.13	13.67	1.65	17.69	0.79	9.48	2.37	17.18	0.76	11.45	1.96
B5-Ibs	B	0.6	13.39	19.99	56.55	402	100	100	0	27	30.05	1.11	16.1	1.68	21.37	0.79	11.45	2.36	19.15	0.71	12.77	2.11
B6- Ias	B	0.6	8.13	19.99	56.55	226	100	150	0	29	29.02	1.00	15.55	1.87	22.34	0.77	11.97	2.42	22.58	0.78	15.05	1.93
B6-Ibs	B	0.6	8.13	19.99	56.55	402	100	150	0	33.75	32.24	0.96	17.27	1.95	24.59	0.73	13.17	2.56	25.02	0.74	16.68	2.02
Albegmprli (2017)																						
B1-0	B	0.65	4.97	54.00	0	603	150	210	0	54.1	53.43	0.99	28.62	1.89	42.91	0.79	22.99	2.35	31.54	0.58	21.03	2.57
B2-1	B	0.65	9.85	54.00	0	402	150	160	0	45.5	47.93	1.05	25.68	1.77	35.96	0.79	19.26	2.36	26.97	0.59	17.98	2.53
B2-0	B	0.65	9.85	55.10	0	603	150	160	0	58.5	53.37	0.91	28.59	2.05	40.11	0.69	21.49	2.72	31.07	0.53	20.71	2.82
B3-0	B	0.65	14.62	59.00	0	603	150	110	0	54.5	53.35	0.98	28.58	1.91	37.40	0.69	20.04	2.72	25.89	0.47	17.26	3.16
B3-1	B	0.65	14.62	52.00	0	402	150	110	0	55.5	44.50	0.80	23.84	2.33	30.45	0.55	16.31	3.40	21.69	0.39	14.46	3.84
El-Niema (1988)																						
T1	B	0.9	9.45	21.80	0	625	100	110	0	58	50.48	0.87	27.04	2.14	19.07	0.33	10.22	5.68	14.35	0.25	9.57	6.06
T2	B	0.9	4.76	27.60	0	625	100	185	0	69.5	65.96	0.95	35.34	1.97	21.03	0.30	11.27	6.17	18.38	0.26	12.25	5.67
T1-1	B	0.9	9.45	23.30	0	625	100	110	0	47.5	42.33	0.89	22.68	2.09	19.35	0.41	10.37	4.58	14.67	0.31	9.78	4.86
T2-2	B	0.9	4.76	23.70	0	625	100	185	0	63	51.96	0.82	27.84	2.26	19.89	0.32	10.66	5.91	17.47	0.28	11.65	5.41
Debaiky and El-Niema (1982)																						
A4	C	0.9	-4.76	22.00	47.5	942	120	335	0	51.3	49.31	0.96	26.42	1.94	35.10	0.68	18.80	2.73	38.13	0.74	25.42	2.02
C5	C	0.9	-4.76	31.40	47.5	942	120	335	0	57.5	54.85	0.95	29.38	1.96	39.01	0.68	20.90	2.75	40.37	0.70	26.91	2.14
E2	C	0.9	-4.76	33.50	56.6	603	120	335	0	75	70.98	0.95	38.03	1.97	52.97	0.71	28.38	2.64	49.48	0.66	32.99	2.27
A5	C	0.9	-9.46	22.50	47.5	942	120	410	0	57	48.02	0.84	25.73	2.22	22.48	0.39	12.04	4.73	34.78	0.61	23.19	2.46
C4	C	0.9	-9.46	31.10	47.5	942	120	410	0	61	53.70	0.88	28.77	2.12	25.46	0.42	13.64	4.47	36.21	0.59	24.14	2.53
D5	C	0.9	-9.46	28.90	47.5	942	120	410	0	65	79.73	1.23	42.71	1.52	44.78	0.69	23.99	2.71	58.10	0.89	38.73	1.68
D6	C	0.9	-9.46	32.20	101	942	120	410	0	75	85.23	1.14	45.66	1.64	48.38	0.65	25.92	2.89	61.41	0.82	40.94	1.83
E1	C	0.9	-9.46	34.80	56.6	603	120	410	0	95	75.67	0.80	40.54	2.34	43.20	0.45	23.14	4.10	47.34	0.50	31.56	3.01
F1	C	0.9	-9.46	21.10	56.6	603	120	410	0	67	56.02	0.84	30.01	2.23	30.68	0.46	16.44	4.08	36.71	0.55	24.47	2.74
F2	C	0.9	-9.46	20.80	56.6	763	120	410	0	70.5	53.80	0.76	28.82	2.45	28.10	0.40	15.05	4.68	37.52	0.53	25.01	2.82
El-Niema (1988)																						
T4	C	0.9	-4.76	24.30	0	625	100	335	0	88	80.98	0.92	43.38	2.03	29.10	0.36	15.59	5.64	68.26	0.85	45.51	1.93
T5	C	0.9	-9.45	22.70	0	625	100	410	0	81.5	85.49	1.05	45.8	1.78	14.76	0.17	7.91	10.31	14.25	0.16	9.50	8.58
T4-4	C	0.9	-4.76	25.40	0	625	100	335	0	74	62.38	0.84	33.42	2.21	5.55	0.07	2.97	24.89	9.74	0.12	6.49	11.40
T5-5	C	0.9	-9.45	25.00	0	625	100	410	0	75	65.25	0.87	34.96	2.15	15.16	0.20	8.12	9.23	14.46	0.20	9.64	7.78
Tena *et al*. (2008)																						
TASC1-0	C	1.083	-3.07	32.10	0	2025	220	410	0	67.5	80.21	1.19	42.97	1.57	6.26	0.08	3.35	20.13	10.06	0.13	6.71	10.06
TASC2-0	C	1.083	-6.12	29.50	0	2025	220	410	0	60	61.98	1.03	33.2	1.81	34.29	0.57	18.37	3.27	35.93	0.60	23.95	2.50
TASC3-0	C	1.083	-9.13	23.60	0	2025	220	410	0	37.5	39.09	1.04	20.94	1.79	5.22	0.14	2.80	13.41	20.66	0.55	13.77	2.72
TASC4-0	C	1.083	-12.10	28.10	0	2025	220	410	0	30	27.88	0.93	14.94	2.01	-14.58	-0.49	-7.81	-3.84	7.92	0.26	5.28	5.68

Mehmet Eren Gulsan, Hasan M. Albegmprli and Abdulkadir Cevik

Table A.1 Continued

Tena *et al.* (2008)																						
TASC1-1	C	1.083	-3.07	26.90	100.5	2025	220	410	0	200	162.01	0.81	86.79	2.3	139.53	0.70	74.75	2.68	123.08	0.62	82.05	2.44
TASC2-1	C	1.083	-6.12	29.20	100.5	2025	220	410	0	170	146.28	0.86	78.36	2.17	103.42	0.61	55.40	3.07	105.51	0.62	70.34	2.42
TASC3-1	C	1.083	-9.13	28.80	100.5	2025	220	410	0	120	125.63	1.05	67.3	1.78	66.80	0.56	35.79	3.35	87.09	0.73	58.06	2.07
TASC4-1	C	1.083	-12.10	21.10	100.5	2025	220	410	0	80	94.01	1.18	50.36	1.59	29.10	0.36	15.59	5.13	68.26	0.85	45.51	1.76
Albegmprli (2017)																						
C2-0	C	0.65	-9.85	44.00	0	603	150	310	0	38.9	37.46	0.96	20.07	1.94	23.03	0.59	12.34	3.15	13.78	0.35	9.19	4.23
C3-0	C	0.65	-14.62	62.00	0	603	150	360	0	37.15	40.60	1.09	21.75	1.71	16.30	0.44	8.73	4.25	8.47	0.23	5.65	6.58
C1-0	C	0.65	-4.97	58.50	0	603	150	260	0	39.3	44.09	1.12	23.62	1.66	39.60	1.01	21.21	1.85	22.30	0.57	14.87	2.64
C2-1	C	0.65	-9.85	61.00	0	402	150	310	0	37.15	46.64	1.26	24.99	1.49	30.25	0.81	16.21	2.29	13.42	0.36	8.95	4.15
C3-1	C	0.65	-14.62	51.00	0	402	150	360	0	33.6	39.12	1.16	20.96	1.6	17.44	0.52	9.34	3.60	6.94	0.21	4.63	7.26
Average												0.96		2.00		0.81		3.35		0.66		2.88
COV												0.14		0.16		0.4		1.11		0.26		0.68